IOP Conf. Series: Journal of Physics: Conf. Series **1252** (2019) 012007 doi:10.1088/1742-6596/1252/1/012007

Thermodynamic analysis of semiflexible helical polymers

Matthew J. Williams

E-mail: mjw532@uga.edu
Institute of Engineering, Murray State University, Murray, KY 42071, USA

Michael Bachmann

E-mail: bachmann@smsyslab.org
Soft Matter Systems Research Group, Center for Simulational Physics, The University of Georgia, Athens, GA 30602, USA

Abstract. Tertiary structure formation underlies the folding mechanics of many classes of polymers. A simplified model of helical polymers is a useful system in which to begin studying the formation and properties of compact conformations known from biomolecules. Hyper-phase diagrams and structural transitions are presented for polymers of length 40 and 50 over an array of model parameters.

1. Introduction

In biological polymers, helical structures are a result of hydrogen bonding along the polymer backbone or by an ordering principle such as many-body constraints [1, 2, 3]. Similar structures can be simulated in generic homopolymer systems by using a carefully chosen model [4, 5, 6, 7]. In these decidedly finite systems, structural changes are not phase transitions in the strict thermodynamic sense [8, 9]. However, biologically relevant macromolecules operate on mesoscopic scales and the finite-size effects are interesting and should be considered in the thermodynamic interpretation of structural transitions [10]. To understand helical polymer systems we analyze the transitions in temperature and model parameter space, the folding dynamics and stability, and conformation geometry [11, 12, 13]. For this purpose, extensive parallel-tempering Monte Carlo Simulation were performed.

2. Model

For the study of helical homopolymers we include in our model four essential effective potentials. Interaction between bonded monomers separated by a distance r is described by the FENE potential, $v_{\rm bond}(r) = \log\{1-[(r-r_0)/R]^2\}$. The minimum of this potential occurs at a distance $r_0 = 1$ and $R = (3/7)r_0$ represents half of the width of the well. The Lennard-Jones potential describes the interaction between any two non-bonded monomers separated by a distance of r. This potential is given by the expression $v_{\rm LJ}(r) = 4[(\sigma/r)^{12} - (\sigma/r)^6] - v_c$, where $\sigma = 2^{-1/6}r_0$. The computational efficiency can be greatly increased with no appreciable influence on structure formation by considering all non-bonded interactions of distance $r > r_c = 2.5\sigma$ to have no energy

contribution. To avoid a discontinuity in the potential we include a shift in the Lennard-Jones energy of $v_c = 4[(\sigma/r_c)^{12} - (\sigma/r_c)^6]$.

Helical order is provided by a torsion potential which provides an energy penalty for any torsion angle τ, which differs from reference angle $\tau_0 = 0.873$ radians: $v_{\rm tor}(\tau) = 1 - \cos(\tau - \tau_0)$. Helical segments are provided stability by inclusion of a bending potential which penalizes bending angles θ deviating from a reference bending angle $\theta_0 = 1.742$ radians. The bending potential is $v_{\rm bend}(\theta) = 1 - \cos(\theta - \theta_0)$.

These four potentials are each scaled by a pre-factor which determines their relative strength. Thus, the total energy of a polymer confirmation $\mathbf{X} = (\mathbf{x}_1, \mathbf{x}_2, ..., \mathbf{x}_N)$ is given by

$$E(\mathbf{X}) = S_{\rm LJ} \sum_{i>j+1} v_{\rm LJ}(r_{ij}) + S_{\rm bond} \sum_i v_{\rm bond}(r_{i\,i+1}) + S_\theta \sum_k v_{\rm bend}(\theta_k) + S_\tau \sum_l v_{\rm tor}(\tau_l). \qquad (1)$$

The energy scales used in this study are $S_{\rm LJ} = 1$, $S_{\rm bond} = -KR^2/2$ where $K = (98/5)$ and r_0^2 and $R = (3/7)r_0$, $S_\theta = 200$. The torsion strength S_τ is varied to achieve different helix bundling. In this study, we focus on polymer chains with $N = 40$ and 50 monomers.

3. Simulation

To simulate these systems we executed a 32-thread parallel tempering simulation with temperatures between $T = 0.03$ and 2.5. Each thread performed 400 updates per attempted thread exchange. Two update types were used in these simulations. Most updates were displacement updates.

For each displacement update, a random monomer is chosen and a new location is proposed for that monomer inside of a box of side length r_d surrounding its original location. The change

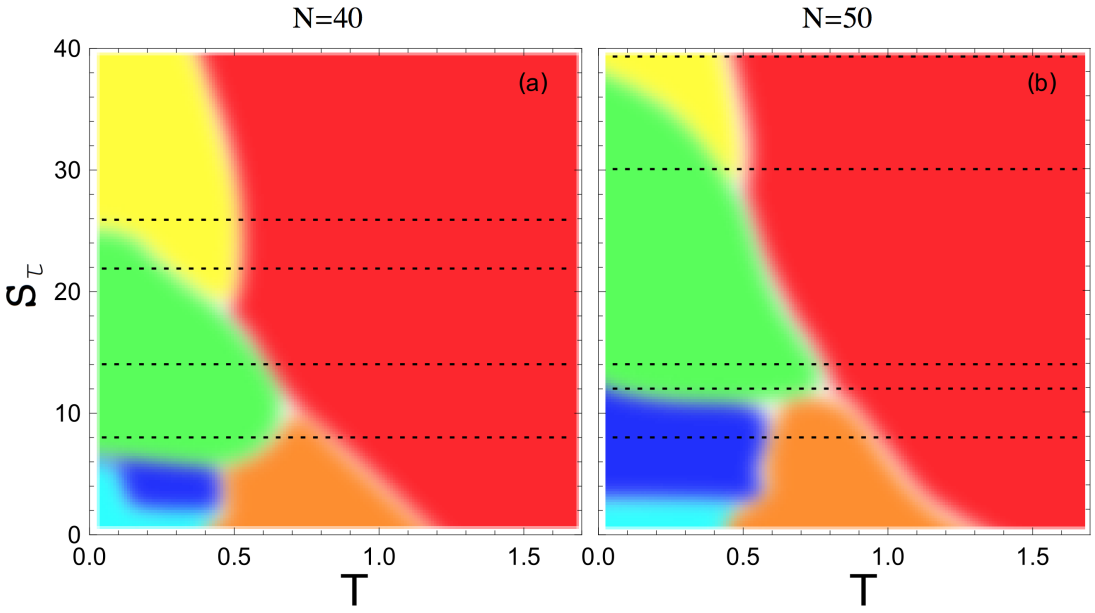

Figure 1. The parameter space under which different structure types are formed for polymers with $N = 40$ (a) and $N = 50$ (b). Dashed lines represent S_τ values which will be explored further in the rest of the paper.

in energy of the polymer, ΔE, is calculated, and the move is accepted with probability

$$P_{\text{accept}} = \begin{cases} e^{-\beta_i \ \Delta E}, & \text{if } \Delta E > 0 \\ 1, & \text{otherwise,} \end{cases} \tag{2}$$

where β_i is the inverse temperature in the i-th thread. The size of the box has a not insignificant impact on the efficiency of the simulation and is chosen in such a way as to cause displacement updates to be accepted approximately half of the time.

For every $3N$ displacement updates a torsion update is attempted. To perform a torsion update, a random bond and a random rotation angle is chosen. Every monomer following the bond is rotated by the chosen angle. This changes one torsion angle without changing any other aspects of the structure. This move is also accepted or rejected according to the criterion given in Eq. 2.

For each exchange, simulation threads attempt to trade replicas with neighboring threads. Exchanges are accepted with probability $P_{\text{accept}} = \min(1, e^{-(\beta_i - \beta_j)(E_j - E_i)})$ [14, 15, 16].

4. Hyperphase diagrams

Simulations are preformed for S_τ varying between 0 and 30 for polymers of length $N = 40$ and S_τ between 0 and 50 for polymers of length $N = 50$. From the results of each simulation, structural transitions are found by observing the average energy $\langle E \rangle$ and the specific heat C_v

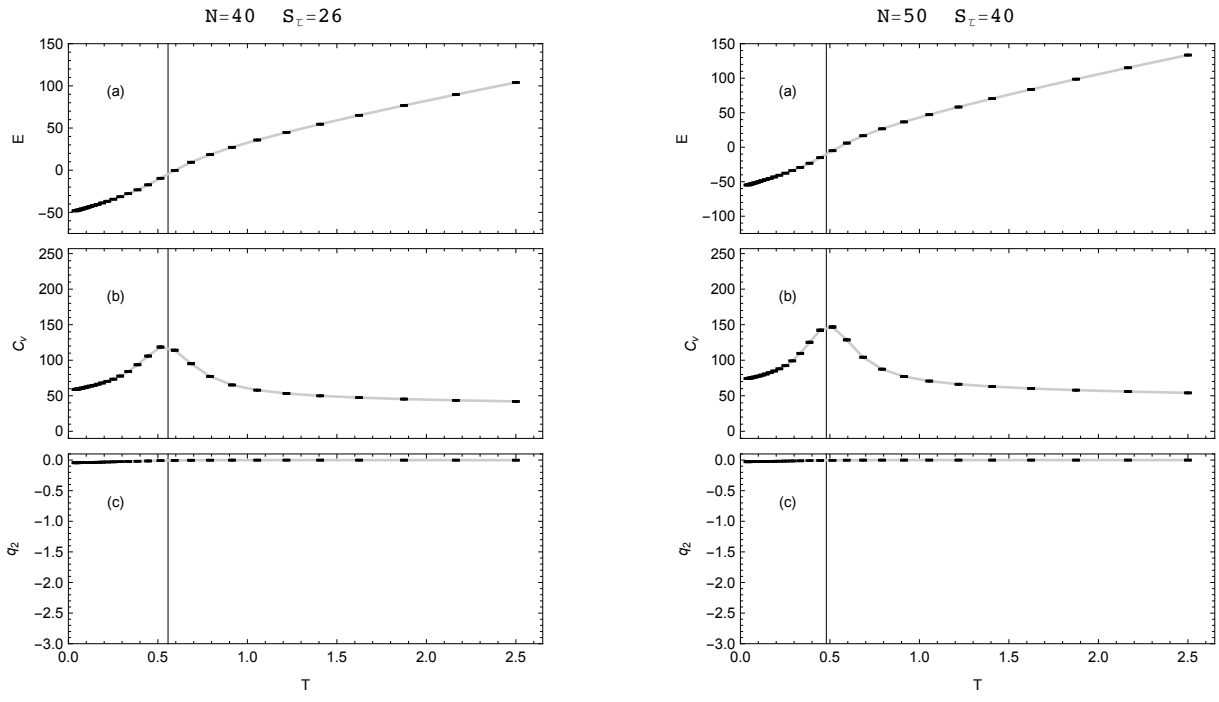

Figure 2. Energy, specific heat, and q_2 as functions of temperature for the 40-mer with $S_\tau = 26$ is given on the left and the same parameters for $N = 50$ and $S_\tau = 40$ is given on the right. In both cases a single transition between the single-helix phase and the random-coil phase is clearly seen in the specific heat plot. For both the single helix and random coil, there is very little interaction between monomers which are separated by more than 6 bonds and q_2 is therefore nearly 0 in both cases. The vertical line in each panel represents the temperature at which the structural transition occurs.

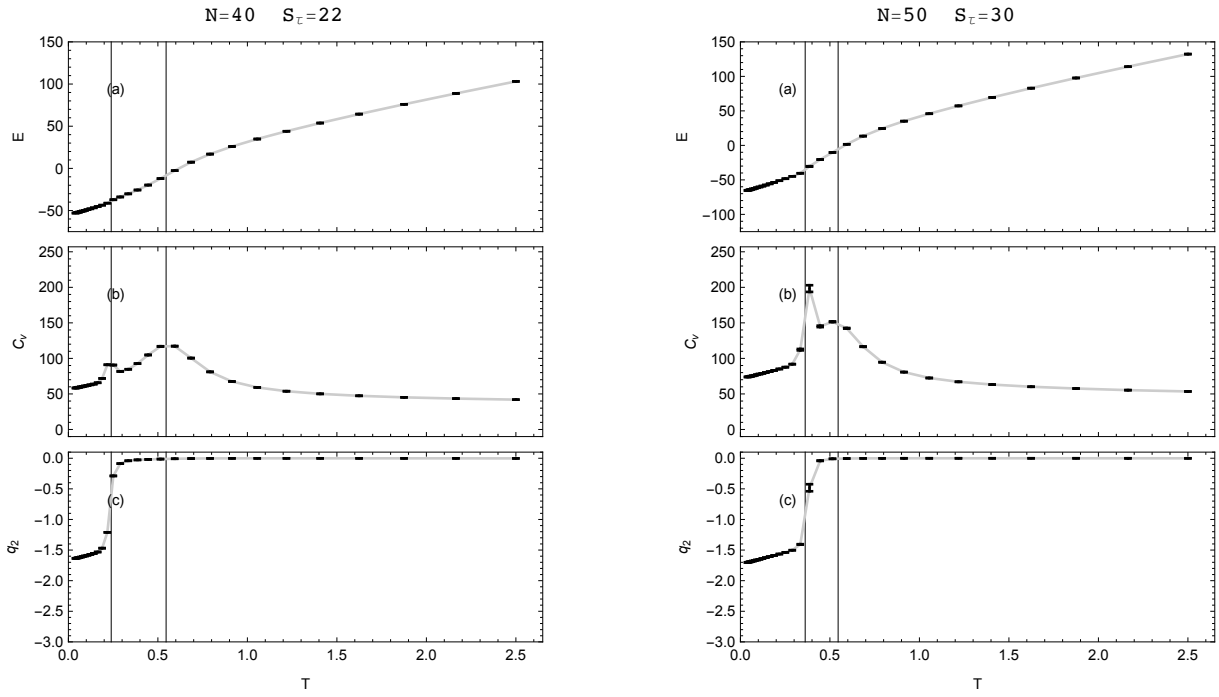

Figure 3. Energy, specific heat, and q_2 as functions of temperature for the 40-mer with $S_\tau = 22$ is given on the left and the same parameters for $N = 50$ and $S_\tau = 30$ is given on the right. In both cases the high-temperature phase is governed by random coils. As temperature decreases, both systems show a broad transition peak representing the transition from random coils into the single-helix phase and then a sharper peak in C_v corresponding to the transition from single helix to two-helix bundles. The two-helix bundle phase is apparent in the q_2 parameter because once the polymer is folded the magnitude of the interaction between monomers separated by more than 6 bonds increases drastically. The vertical lines in each panel represent the temperatures at which the structural transition occurs.

as functions of the temperature of the system. An additional structure parameter q_2 is found to be useful in distinguishing various bundling configurations. This parameter is defined as the average over all monomers of their LJ interaction with all other monomers separated from them by more than 6 bonds. This parameter can be calculated from the equation

$$q_2(\mathbf{X}) = \epsilon \frac{1}{N} \sum_{i=1}^{N-2} \sum_{j=i+2}^{N} \Theta_{j-i,7}\, v_{\mathrm{LJ}}(r_{ij}), \tag{3}$$

where $\Theta_{k,\ell} = 1$ if $k \geq \ell$ and 0 otherwise.

From these simulations we find that various different structure types are formed. At high temperature, structures lack order and are considered to be in the random-coil phase. Confirmations often transition into liquid phases as they cool. At low temperature, polymers form more organized global structures made up of helical segments. These include single helices, two-helix bundles, and three-helix bundles. If insufficient torsion potential is provided, polymers cease to form helical segments and instead form amorphous solid structures. The conditions under which each of these structure types is formed is provided by the hyperphase diagram shown in Fig. 1.

For specific example values of S_τ we will provide further data supporting the choice of transition temperature.

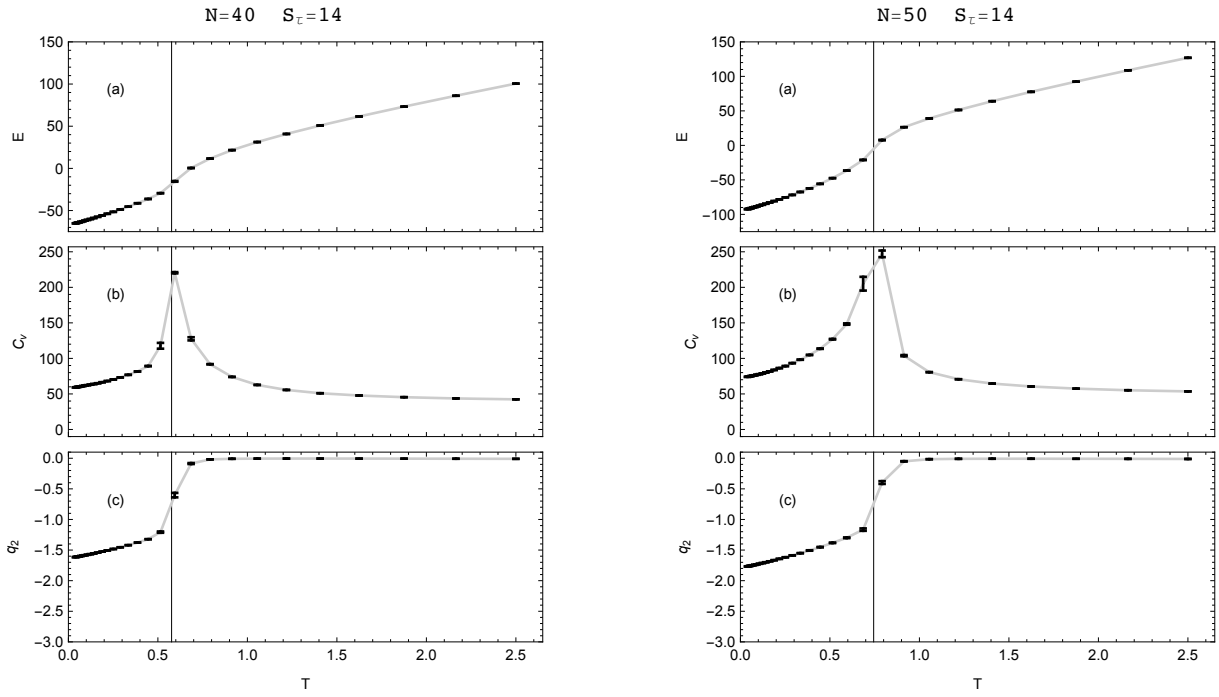

Figure 4. Energy, specific heat, and q_2 as functions of temperature for the 40-mer with $S_\tau = 14$ is given on the left and the same parameters for $N = 50$ and $S_\tau = 14$ is given on the right. In both cases the high-temperature phase is random coil and at low temperatures the two-helix bundles dominate. There is a single transition occurring between the two phases which is visible in both the specific heat and q_2.

4.1. Random coil - single helix transitions

For large values of S_τ polymers tend to form single helices at low temperature and random coil structures at higher temperature with one obvious structural transition in between. In the $N = 40$ polymer, this occurs for values at or above $S_\tau = 26$. At this threshold value, the transition is found at about $T = 0.56$. Similar behavior is observed for the $N = 50$ polymer at $S_\tau = 40$ with the transition temperature at a slightly lower value of $T = 0.48$. For both $N = 40$ and $N = 50$ the transition between single helix and random-coil phase can be clearly seen in Fig. 2.

If S_τ is increased further, no new structure types occur, but the transition temperature decreases.

4.2. Random coil - single helix - two-helix bundle transitions

There are values of S_τ for which both two-helix bundles and single helices occur: $18 < S_\tau < 26$ for $N = 40$ and $29 < S_\tau < 40$ for $N = 50$. In this domain, the two-helix bundle is dominant at a lower temperature than the single helix. The transition between the single helix and random-coil phase occurs in much the same way as the previous example but at lower temperatures, a new sharper transition appears in the specific heat curves as seen in Fig. 3. This new transition corresponds to the transition between single-helix structures and two-helix bundles.

The q_2 parameter becomes very useful in distinguishing between the structure types. When a long single helix is folded in half, new contacts are formed between monomers separated by more than 6 bonds and q_2 decreases.

4.3. Random coil - two-helix bundle transitions
At values of $S_\tau < 18$ for $N = 40$ and $S_\tau < 29$ for $N = 50$, there is no longer any temperature for which single-helix phases dominate. We see only a single strong transition between the two-helix phase and the random-coil phase in this regime. For both $N = 40$ and $N = 50$ we present data at $S_\tau = 14$ in Fig. 4. It is unsurprising that the transition occurs at a higher temperature for the polymer of length 50. For the longer polymer, the energetic benefit to folding is also larger.

4.4. Three-helix bundle boundary
In the $N = 50$ system at $S_\tau = 12$ we are on the boundary between two-helix bundles and three-helix bundles at low temperature. The energy, specific heat, and q_2 are given as functions of temperature in Fig. 5. Here, there is an obvious transition between the random-coil phase and the two-helix bundle phase at $T = 0.8$ and an additional low temperature transition from two-helix bundle to three-helix bundles at $T = 0.1$. The three phases are very nicely discernible in the q_2 plot. In the random-coil phase, q_2 is approximately 0. Below the two-helix transition point, q_2 stair steps down to a plateau at approximately -1.5. There is an additional stair step at the three-helix bundle transition to a value of approximately -2.75.

4.5. Structure formation for low S_τ
For both polymer lengths at $S_\tau = 8$, we see helix bundles at low temperature and random-coil phase at high temperature. Both systems show an intermediate liquid phase between the two. For the shorter $N = 40$ polymer the low temperature phase is a very clear, stable, two-helix bundle phase much like at $S_\tau = 14$. For the longer polymer ($N = 50$), the low-temperature phase is the three-helix bundle. It is apparent in Fig. 6 (b), that there is an additional solid-solid like transition at a temperature of approximately $T = 0.12$. The structures on either side of this

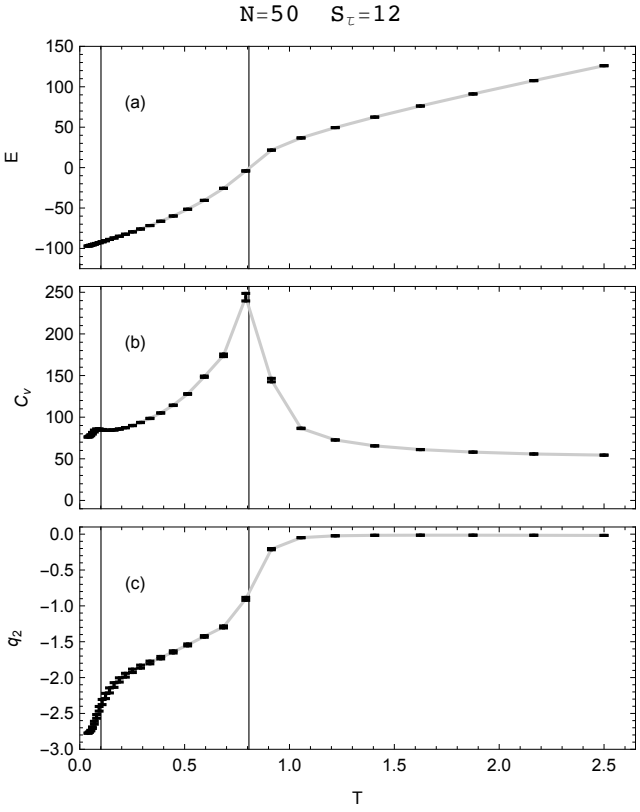

Figure 5. Energy, specific heat, and q_2 across temperature for $N = 50$ and $S_\tau = 12$. Here we are on the boundary between forming two-helix bundles if S_τ were larger and three-helix bundles if S_τ were smaller. In the specific heat curve there are two apparent structural transitions, one at $T = 0.8$ and the other at $T = 0.1$. The pronounced transition signal at $T = 0.8$ is associated with the transition between the random-coil phase and the two-helix phase. At very low temperature, another transition occurs, this time from two-helix bundles to three-helix bundles.

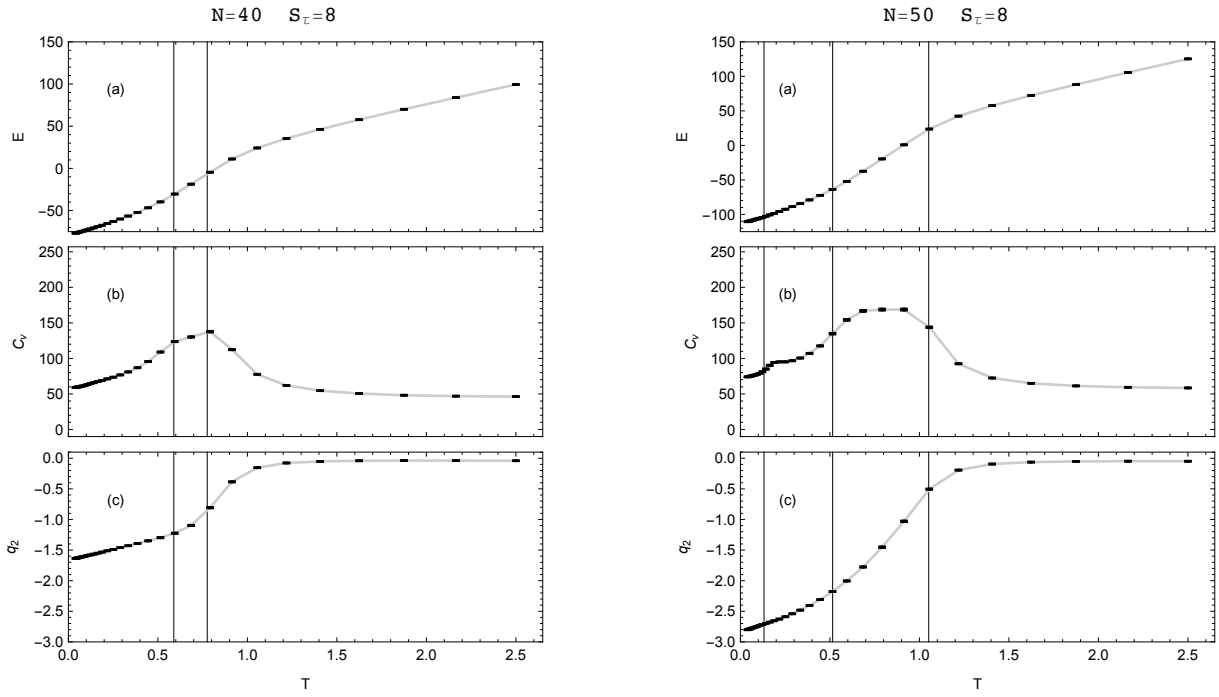

Figure 6. Average energy, specific heat, and q_2 as functions of temperature for $S_\tau = 8$ in polymers of 40 (left) and 50 (right) monomers. For both polymer lengths we find a random-coil phase at high temperatures and helix bundles at low temperature with a liquid phase in between. At length 40, the low temperature phase consists of two-helix bundles and for polymers of length 50 the low temperature phase dominated by three-helix bundles. Interestingly, in the $N = 50$ system specific heat plot there is a very clear transition deep within the three-helix bundle phase. This is a transition between two very similar three-helix bundle structure types with no discernibility in q_2.

transition are both very clearly 3-helix bundles with no visible distinction between the two.

5. Conclusion

Plots of canonical averages of energy, specific heat, and q_2 parameter can be useful in distinguishing phase transitions in coarse-grained models for helical homopolymers. These phase transitions can then be used to generate a hyper-phase diagram showing regions model space in which different structure types form. In this paper, we presented hyper-phase diagrams for polymers of length $N = 40$ and $N = 50$ across the torsion parameter S_τ and temperature T. We then choose several example values for S_τ for which to present the underlying canonical data for the structures energies, specific heats, and helix bundle parameter q_2. It is apparent that transitions in the canonical data often correspond to qualitative changes in structure type. Depending on the specific parameter choices, these quantities allow for the discrimination of three-helix bundles, two-helix bundles, single helices, amorphous structures, liquid, and random coil phases.

Acknowledgments

This project was supported by NSF Grant No. DMR-1463241.

6. References

[1] Maritan A, Micheletti C, Trovato A and Banavar J R 2000 *Nature* **406**, 287
[2] Kemp J P and Chen Z Y 1998 *Phys. Rev. Lett.* **81**, 3880
[3] Rapaport D C, Johnson J E, and Skolnick J 1999 *Comput. Phys. Commun.* **121-122**, 231
[4] Vogel T, Neuhaus T, Bachmann M and Janke W 2009 *Phys. Rev. E* **30**, 7
[5] Williams M J and Bachmann M 2015 *Phys. Rev. Lett.* **115**, 048301
[6] Williams M J and Bachmann M 2016 *Polymers* **8**, 245
[7] Williams M J and Bachmann M 2016 *Phys. Rev. E* **93**, 062501
[8] Badasyan A V, Giacometti A, Mamasakhlisov Y S, Morozov V F and Benight A S 2010 *Phys. Rev. E* **81**, 021921
[9] Poland D and Scheraga H A 1970 *Theory of Helix-Coil Transitions in Biopolymers: Statistical Mechanical Theory of Order-Disorder Transitions in Biological Macromolecules* (Academic Press)
[10] Bachmann M 2014 *Thermodynamics and Statistical Mechanics of Macromolecular Systems* (Cambridge University Press)
[11] Grosberg A Y and Khokhlov A R 1994 *Statistical Physics of Macromolecules* (AIP Press)
[12] Dill K A and Chan H S 1997 *Nat. Struct. Biol.* **4**, 10
[13] Flory P J 1949 *J. Chem. Phys.* **17**, 303
[14] Swendsen R H and Wang J-S 1986 *Phys. Rev. Lett.* **57**, 2607
[15] Hukushima K, Takayama H, and Nemoto K 1996 *Int. J. Mod. Phys. C* **07**, 337
[16] Geyer C J 1991 *Comput. Sci. Stat. Proc. 23rd Symp. Interface* (Interface Foundation, Fairfax, VA) pp. 156-163